# Mass Transfer in Two-Phase Flow in Horizontal Pipelines

**JOHN C. JEPSEN**

**Shell Development Company, Emeryville, California**

**The objective of the present study was to obatin data on the rate of liquid-phase controlled mass transfer in two-phase gas-liquid flow in horizontal pipes. Studies were made on the effect of the mean gas and liquid flow rate, pipe diameter, and pipe orientation on $k_la$, the mean liquid-phase film mass transfer coefficient. Experimental studies were made on 1 and 4 in. I.D. horizontal pipelines; on 4 in. I.D. 180 deg. vertical short radius bend ($H/D = 2$); and on 3/16, 5/16, and 7/16 in. I.D. tubes wound in 4-in. diameter spirals (upflow). A general correlation is presented for $k_la$ as a function of the two-phase frictional energy dissipation, liquid-phase physical properties, and pipe diameter.**

It has been conjectured for some time that concurrent gas/liquid flow in a pipeline might provide a very efficient means of obtaining good gas/liquid contacting. Applications where such a contactor might be advantageous include absorption or stripping operations which require only one equilibrium stage or a reactor where mass transfer and chemical reaction occur simultaneously. Efficient contacting may require a relatively high pressure loss. The simplicity of the pipeline and the small capital investment will, in many applications, far outweigh the increased pressure loss requirement.

Use of pipeline contactors and reactors in the chemical industry has in the past been limited to special cases because of the lack of data. Interest in pipeline contactors has increased in the last few years, and several papers have recently been published on mass transfer in two-phase flow. Heuss, King, and Wilke (*8*) have reported the rates of absorption of ammonia and oxygen from air into water in horizontal cocurrent gas-liquid froth flow in a 1 in. I.D. pipe. The range of superficial gas and liquid velocities examined were 14 to 50 ft./sec. and 7 to 16 ft./sec., respectively. The rates of absorption were determined from liquid samples withdrawn from the pipeline at distances ranging from 6 to 36 in. downstream from the air/water distributor. Individual gas- and liquid-phase film capacity coefficients were reported. Scott and Hayduk (*7, 14*) studied liquid-phase controlled absorption of pure gases into various liquids in 1.228, 1.757, and 2.504 cm. I.D. horizontal tubes. Carbon dioxide and helium were used as the gas phase and water, and ethanol and ethylene glycol were used as the liquid phase. The range of superficial gas and liquid velocities studied were 0.1 to 20 ft./sec. and 0.5 to 3.6 ft./sec., respectively. Data in the bubble and plug flow regimes were correlated by an equation based on qualitative observations and an analogy to the case of a single flowing fluid. The effects of liquid-phase physical properties were included in the correlation by a multiple regression technique. Wales (*15*) determined overall mass transfer coefficients for annular and dispersed two-phase flow in a horizontal 1 in. I.D. pipe. Systems studied were the desorption of carbon dioxide from water into air and absorption of carbon dioxide from air into dilute sodium hydroxide solutions. Lamont and Scott (*10*) made an experimental study on liquid-phase mass transfer from bubbles traveling concurrently with liquid in a horizontal pipe. The system studied was absorption of pure carbon dioxide into water. Anderson et al. (*1*) measured the rate of absorption of ammonia from air into water in a 1 in. I.D. horizontal pipeline under conditions of annular flow. Superficial liquid and gas velocities were varied from 0.15 to 1.6 ft./sec. and 45 to 240 ft./sec., respectively. Hughmark (*9*) estimated gas- and liquid-phase mass transfer coefficients using a momentum mass transfer analogy. Results of these estimates were compared with experimental results obtained by Anderson (*1*) and by Bollinger (*2*). The five pairs of literature data given above have not been compared by any of the authors.

The objective of our work was to experimentally determine the effect of gas/liquid flow rates, pipe diameter, and pipeline orientation on the rate of liquid-phase controlled mass transfer in concurrent horizontal two-phase flow.

## SCOPE OF EXPERIMENTS

Pressure drop and liquid-phase controlled mass transfer (oxygen absorption and desorption) measurements were made on concurrent air/water flow in the following pipelines: 1 and 4 in. I.D. horizontal pipeline; 4 in. I.D., 180 deg. vertical short radius bend ($H/D = 2.0$); and 3/16, 5/16, and 7/16 in. I.D. tubes wound in 4-in. diameter spirals (upflow).

The range of mean gas and liquid superficial velocities studied are summarized as follows:

| Pipeline | Liquid superficial velocity | Gas superficial velocity |
|---|---|---|
| 1 in. | 1.0 to 7.4 ft./sec. | 2.5 to 36.0 ft./sec. |
| 4 in. | 4.4 to 11.7 ft./sec. | 39.0 to 168.0 ft./sec. |
| Spiral tubes | 0.05 to 1.5 ft./sec. | 1.0 to 15.0 ft./sec. |
| 4 in. I.D., 180 deg. bend | 4.4 to 11.7 ft./sec. | 39.0 to 110.0 ft./sec. |

## EXPERIMENTAL EQUIPMENT

The 1-in. pipeline consisted of 4-ft. Plexiglass sections

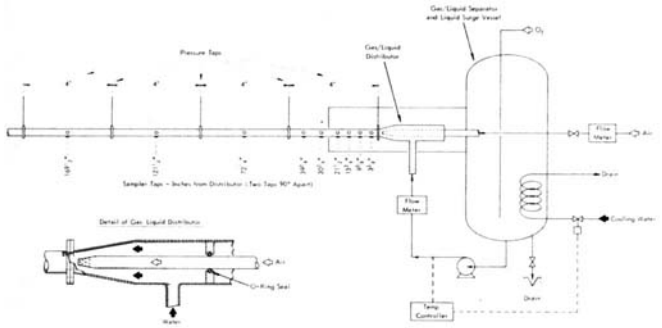

Fig. 1. Schematic diagram 1 in. horizontal pipeline.

coupled together by means of alignment collars. The inside diameters of the collars and the ends of each section of pipe were machined to a common inside diameter (ends of the pipe were tapered) to insure no flow restrictions between sections of pipe. The pipeline was mounted as two parallel 16 ft. horizontal pipes connected together by a U bend. The air and water phases were mixed together with the sparger type of distributor shown in Figure 1. The pipeline was operated with a closed loop system for the liquid phase. The gas/liquid mixture discharging from the 1-in. pipeline passed into 4 in. I.D. by 51 in. long horizontal section and then into a 50-gal. drum which served as a gas/liquid separator and liquid surge vessel. The separated gas phase passed into a gas vent located on top of the drum, and the liquid phase was pumped back into the pipeline by means of a centrifugal pump. The temperature of the liquid phase was controlled to $\pm 0.5°$F. by cooling coils located in the 50-gal. surge vessel. A schematic diagram of the 1-in. pipeline is given in Figure 1.

The 4-in. pipeline consisted of six 6-ft. Plexiglass sections which were aligned and held together in a manner similar to the 1-in. pipeline. The pipeline was operated with a closed loop system for the liquid phase. The gas and liquid phases leaving the pipeline passed through a 4 in., 90 deg. horizontal bend and was then discharged tangentially into a 500-gal. gas-liquid separator and liquid surge vessel. The two phases were separated in the vessel, with the gas phase passing out the top of the vessel through a york mat demister. The liquid phase was removed from the bottom of the vessel through a 10-in. line which was connected in parallel to two 550 gal./min. centrifugal pumps. The discharge from the pumps was connected to the pipeline gas/liquid distributor. No provisions were made for liquid temperature control, as normal heat losses were sufficient to hold the operating temperature around 20°C. Air was obtained from an oil free 2,000 std.cu.ft./min. (100 lb./sq.in. gauge) gear type of air compressor. A schematic diagram of the 4-in. pipeline is given in Figure 2. The 4-in. pipeline gas/liquid distributor is also shown in Figure 2. This distributor differed from the 1-in. pipe distributor in that the liquid and gas phase were injected separately into the bottom and top halves of the pipeline, respectively. The two phases were separated by a liquid tight, flat horizontal plate for a distance of 19 in. downstream from the distributor. This type of distributor rather than the sparger type of distributor was used to minimize entrance effects. Mass transfer studies on two-phase flow around a 180 deg. vertical bend were made by installing a combination vertical and horizontal 180 deg. short radius bend section in the 4 in. horizontal pipeline. The 180-deg. bend section was installed about 9 ft. downstream from the air/water distributor. The section consisted of a 180 deg. vertical bend, a 6 ft. horizontal section, and a 180 deg. horizontal bend.

The spiral tube contactors consisted of 3/16, 5/16, and 7/16 in. I.D. Tygon tubes coiled around a 4-in. diameter cylinder. The lengths of the tubing were approximately 25 ft. Air and water were distributed in the tubing by a standard tee which was located about 2 ft. upstream from the start of the spiral. The spiral tube contactors were operated with a closed loop system for the liquid phase. The gas and liquid phases leaving the contactor were discharged into a 30-gal. gas/liquid separator and liquid surge vessel identical to the gas/liquid separator and surge vessel used with the 1-in. pipeline. A schematic drawing of the spiral tube contactor is given in Figure 3.

Pressure drop measurements in the various pipelines were made with manometers connected to pressure taps located in the pipelines. Mercury was used as the manometer fluid and water as the pressure transmitting fluid. All lines were back-flushed with water before measurements were made.

Liquid-phase controlled mass transfer studies were made by absorbing and desorbing oxygen. Oxygen rich water for the desorption studies was obtained by sparging oxygen into the liquid surge vessels or piping connecting the liquid centrifugal pumps with the air/water distributor. Oxygen absorption studies were made by operating the pipeline at high pressures (50 to 90 lb./sq.in. gauge) and absorbing oxygen from air into oxygen lean water (water in equilibrium with air at atmospheric conditions). The rate of transfer of oxygen was determined by continuously withdrawing liquid samples from the pipelines and by determining the oxygen concentration with a Beckman model 160 physiological gas analyzer. Oxygen concentration measurements were made at pressures within 5 lb./sq.in. of the pipeline pressure to minimize degassing of the samples. Liquid samples were withdrawn from the 1- and 4-in. pipelines by means of sampler tubes placed vertically in the pipeline through sample taps located on the bottom of the pipe. The inlet end of the sampler tube was cut at a 45-deg. angle, and the tube was oriented so that the cut faced into the direction of flow. The liquid leaving the sampler tubes was fed into a Plexiglass block which contained the oxygen analyzer macroelectrode and a thermocouple. The sampler tube was connected to the electrode holder by means of intramedic polyethylene tubing which allowed visual observation of the liquid sample. The liquid sampling rate was controlled by a ⅛-in. needle valve located on the discharge side of the macroelectrode holder. The sampling rate was adjusted so as to reduce gas entrainment to an insignificant level. A schematic diagram of the liquid sampler is given in Figure 4.

Liquid-phase oxygen concentration measurements indicated no significant radial (vertical axis) oxygen concentration profiles in the 1-in. pipeline. However, rather severe radial pro-

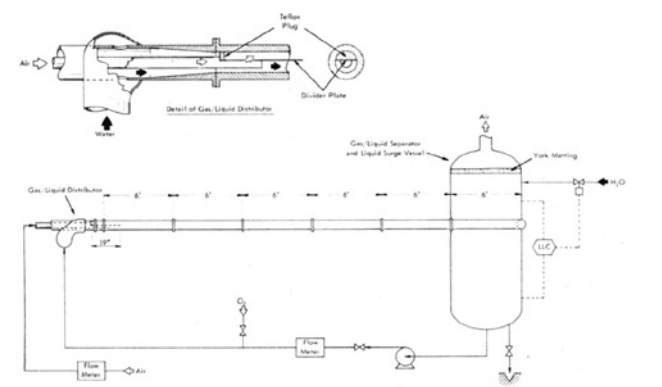

Fig. 2. Schematic diagram 4 in. horizontal pipeline.

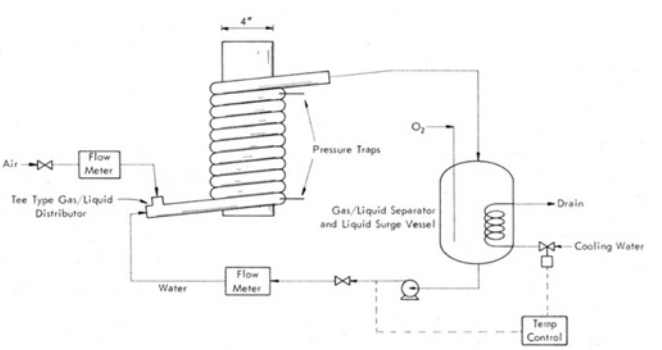


Fig. 3. Schematic diagram spiral tube contactor.

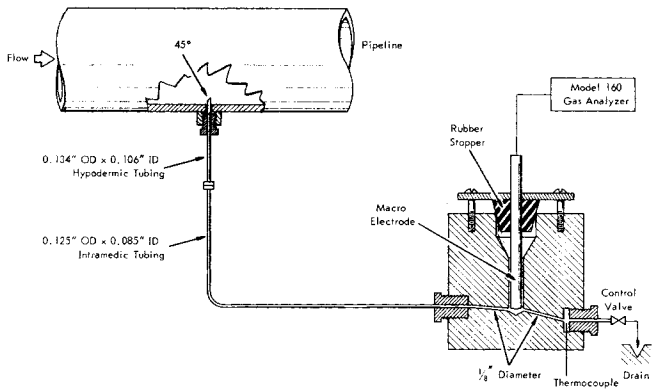


**Fig. 4. Horizontal pipeline liquid sampler and oxygen analyzer macro-electrode holder.**

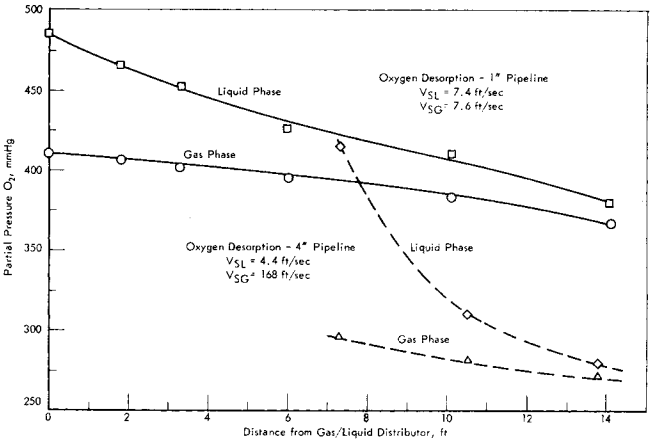


**Fig. 5. Typical axial gas- and liquid-phase oxygen concentration profiles, 1 and 4 in. horizontal pipelines.**

files were found to exist in the 4-in. pipe, which made necessary radial measurements of both oxygen concentration and liquid volumetric flux profiles. Measurement of the radial liquid volumetric flux profiles were made by opening to the atmosphere the discharge end of the liquid sampling probe and by measuring the volume of liquid per unit time which was withdrawn from the pipeline. The measured volumetric liquid fluxes represented time averaged superficial volumetric flows at the sampling points. These samples were not isokinetic but were a fair approximation to the actual isokinetic flows. A detailed discussion of this technique is given in references 5 and 6.

Oxygen concentrations in the spiral tube contactors were measured by inserting a Beckman microelectrode (mounted inside a hypodermic tube) directly into the tubes at known distances from the gas/liquid distributor.

## EXPERIMENTAL RESULTS

### Liquid-phase Controlled Mass Transfer

Mass transfer results were evaluated in terms of $k_la$, the liquid-phase film capacity coefficient, by means of Equation (1):

$$k_la = \frac{V_{SL}}{Z_2 - Z_1}\int_{p_1}^{p_2}\frac{dp}{p_{air} - p} \qquad (1)$$

Evaluation of Equation (1) was made by numerical integration when conditions for analytical solutions were not satisfied. Results of the 1 and 4 in. horizontal pipeline, the 4 in. vertical 180-deg. bend, and the spiral tube studies are filed.* Pipe lengths used in evaluating $k_la$'s in the 1 and 4 in. horizontal pipelines, the 4 in. 180 deg. vertical bend, and the spiral tube contactors were approximately 14, 6, 7, and 14 ft., respectively. Data were taken at several points along each pipeline. The resultant $k_la$ values are not a function of location in the pipelines, as care was taken to insure that entrance effects were insignificant and that superficial gas and liquid velocities did not change appreciably in the measurement section. Typical axial gas and liquid phase oxygen concentration profiles measured on the 1 and 4 in. horizontal pipelines are given in Figure 5.

Evaluation of the results of the oxygen desorption and absorption studies in the 4-in. pipeline were complicated by the presence of radial liquid-phase oxygen concentration profiles. For the case of oxygen desorption, the highest liquid-phase oxygen concentrations occurred near the wall of the pipe, with the minimum occurring slightly above the center line of the pipe (location of minimum liquid flux).

For the case of oxygen absorption, the exact opposite occurred, with the maximum oxygen concentration occurring near the center of the pipe and the minimum near the wall. In most cases, equilibrium conditions between the gas and liquid were approached in the high velocity gas core. The existence of approximately equilibrium conditions in the gas core implies that the rate of mass transfer must be dependent to a large extent on the rate of radial mixing of the liquid phase. These observations are consistent with Anderson's gas-phase controlled mass transfer model (*1*).

Evaluation of the 4-in. pipe data was made by assuming that the partial pressure of oxygen in the air was dependent only on the pressure of the system. [The low solubility of oxygen in water (*12*) results in a negligible transfer of oxygen from the gas phase.] The partial pressure of oxygen in the liquid phase was assumed to be the average liquid-phase partial pressure. An accurate evaluation of the average liquid-phase oxygen concentration was not possible, as concentration and flux profiles were measured only along the vertical radial axis of the pipe. The liquid flux measurements were not isokinetic measurements

| Liquid Phase Oxygen Partial Pressure, mmHg | Liquid Flux, cc/min |
|---|---|
| 630 | 14.9 |
| 645 | 5.35 |
| 580 | 11.5 |
| 455 | 18.4 |
| 410 | 20.9 |

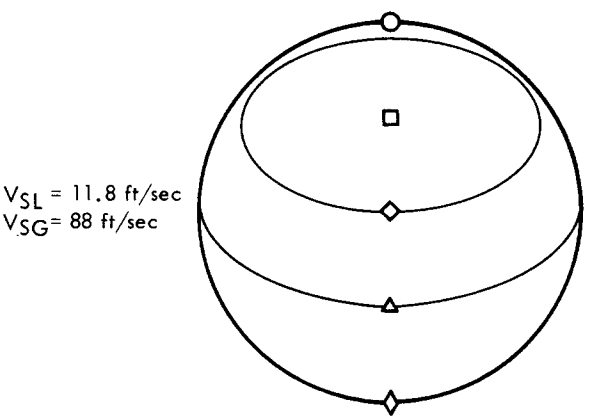


**Fig. 6. Liquid-phase oxygen and flux distribution, 4 in. horizontal pipeline absorption of oxygen from air into water.**

* Material has been deposited as document 00937 with the ASIS National Auxiliary Publications Service, c/o CCM Information Sciences, Inc., 22 W. 34th St., New York 10001 and may be obtained for $1.00 for microfiche or $3.00 for photocopies.

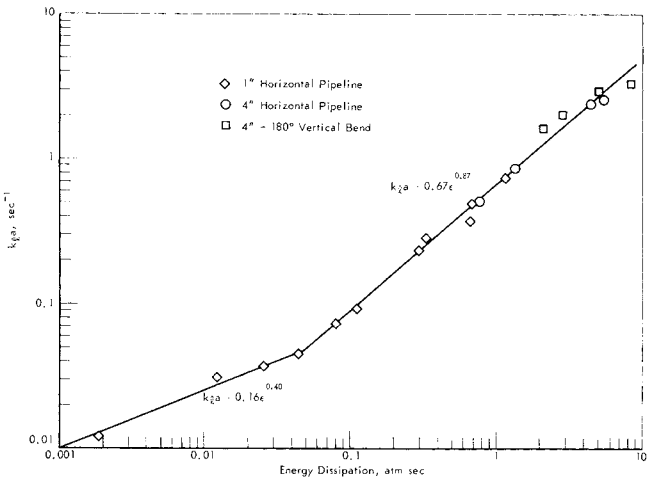


**Fig. 7. Correlation of 1 and 4 in. horizontal pipeline and 4 in. vertical 180-deg. bend liquid film capacity coefficient data.**

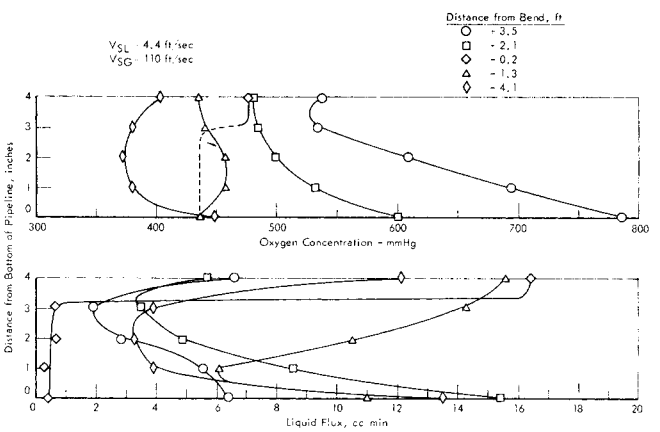


**Fig. 8. Typical radial (vertical axis) liquid flux and liquid-phase oxygen concentration profiles, 4 in. I.D. 180 deg. vertical bend.**

and thus only approximated the distribution of the liquid phase. Estimations of the average concentration were made by drawing contour maps of the liquid flux and oxygen concentrations around the vertical radial axis of the pipe and by numerically integrating the resultant profiles to obtain the average oxygen concentrations. The contour maps of the liquid flux and oxygen concentration were prepared by drawing contour lines representing constant liquid flux or oxygen concentration through the measured data points along the vertical axis. A mirror image type of symmetry of the contour lines was assumed to exist on both sides of the vertical axis. Values for the liquid flux and oxygen concentrations away from the vertical axis were estimated from visual observation of the radial distribution of the phases. Typical liquid flux and oxygen concentration contour maps are given in Figure 6.

Evaluation of $k_la$ values from the 4 in. I.D., 180 deg. vertical bend oxygen desorption data was made by numerically integrating Equation (1). Evaluation of the average liquid-phase oxygen concentration at each sample point was made in the same manner as was used with the 4 in. horizontal pipeline data. The values used for $Z_2 - Z_1$ were the actual distance between sample points as measured along the center line of the pipe.

### Pressure Drop

Frictional pressure losses in the 1 and 4 in. horizontal pipes and the spiral tube contactors were satisfactorily correlated by the Lockhart-Martinelli correlation (*11*). The spiral tube single-phase pressure drops were calculated by using White's friction factor correlation (*16*) for single-phase flow in helical coils.

## DISCUSSION

Results of the 1 and 4 in. horizontal pipeline and the 4 in. I.D., 180 deg. vertical bend mass transfer studies expressed as $k_la$'s were correlated with $\epsilon$, a type of two-phase frictional energy dissipation per unit volume of pipe. The frictional energy dissipation is defined by Equation (2):

$$\epsilon = (\Delta P/\Delta L)_{TPf}\,(V_{SG} + V_{SL}) \qquad (2)$$

The use of frictional energy dissipation for correlating the mass transfer data was made on the basis of its success in correlating gas-liquid stirred tank data (*3, 4*) and concurrent gas/liquid downflow packed bed data (*13*). The use of the energy dissipation defined by Equation (2) is not the result of a theoretical development but is simply based on the fact that it correlates the mass transfer data. This correlation apparently results from the fact that the interfacial area between phases is related to the two-phase frictional pressure loss and the superficial velocities of the phases. It is impossible at this time to defend this correlation theoretically, as there are no experimental data available on what actually occurs locally in most of the concurrent two-phase flow regimes. The only justification which can be given is that it works.

Correlation of the data is shown in Figure 7. As can be seen in Figure 7, all of the data are well correlated by

$$k_la = A\epsilon^B \qquad (3)$$

where $A$ and $B$ are empirical constants. This is rather remarkable, as the data plotted in Figure 7 are for a wide range of gas and liquid flow rates which correspond to flow regimes ranging from bubble flow to mist annular flow, a factor of 4 variation in pipe diameter and flow in both horizontal pipes and around a 180 deg. vertical bend. The energy dissipation used in correlating the vertical bend data is the same as was used in the correlation of the horizontal pipe data. The two-phase frictional pressure loss, however, is not the straight pipe pressure drop but is the measured pressure drop around the vertical bend less the static head of liquid in the pipe. The effect of the 180-deg. bend on the radial liquid-phase oxygen and flux profiles (measured along the vertical axis of the pipe) is shown in Figure 8.

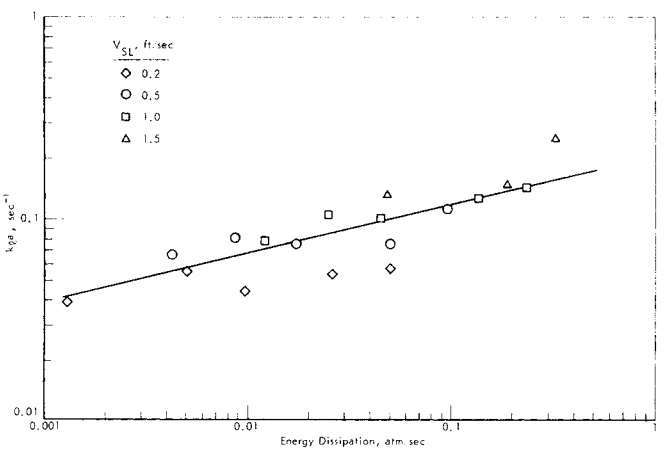


**Fig. 9. Correlation of 3/16 in. I.D. 4-in. diameter spiral tube liquid film capacity coefficient data.**

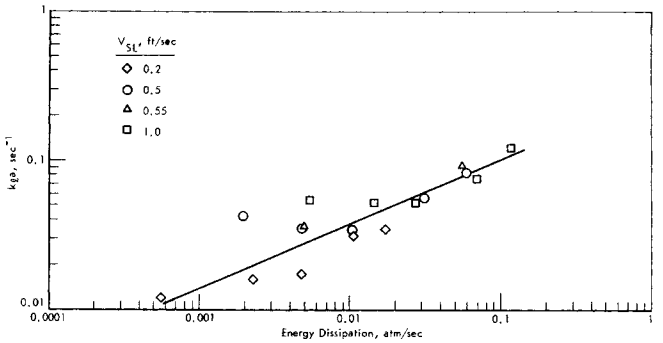


**Fig. 10. Correlation of 5/16 in. I.D. 4-in. diameter spiral tube liquid film capacity coefficient data.**

With reference to Figure 7 again, it is seen that a change in the slope of the correlation occurs at an energy dissipation of about 0.05 atm./sec. This change in slope appears to be related to a change in the hydrodynamics. The relationship, however, is not known.

The spiral tube mass transfer data expressed as $k_l a$'s were also correlated by the two-phase frictional energy dissipation per unit volume of tube. Correlations of the data are shown in Figures 9, 10, and 11. The large amount of scatter (as compared with the results obtained on the 1- and 4-in. pipelines) in the data is believed to be the result of experimental errors.

Comparison of the results of the spiral tube and 1-in. horizontal pipeline studies indicated $k_l a$ to be a function of pipe diameter for energy dissipation of less than 0.05 atm./sec. Results of the 1 and 4 in. horizontal pipe and 4 in. I.D. 180-deg. vertical bend studies indicated no dependency of $k_l a$ on the pipe diameter for energy dissipation greater than or equal to 0.05 atm./sec.

The successful correlation of the mass transfer data by Equation (3) provides a means of evaluating mass transfer data which are available in the literature. Comparison of the $k_l a$ energy dissipation data of Heuss (*8*) with the 1-in. pipe data given in Figure 7 indicated for the same energy dissipation that Heuss' $k_l a$'s are about a factor of 10 larger than the values determined in this study. The apparent discrepancy between data is believed to be the results of entrance effects. In Heuss' study, the rate of oxygen absorption was determined from liquid samples withdrawn batch-by-batch from the pipeline at distances ranging from 6 in. to 3 ft. downstream from the air/water distributor. Results obtained in our study have indicated that entrance effects may persist up to 40 pipe diameters downstream from the distributor, particularly with the distributor design used in Heuss' study. Heuss data probably are valid for the so-called *froth flow regime* which assumes uniform distribution of the phases in the pipeline.

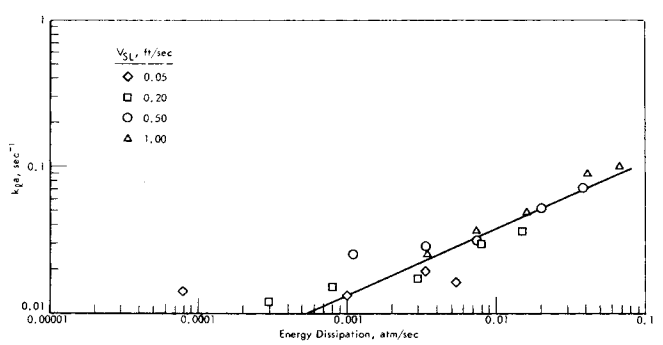


**Fig. 11. Correlation of 7/16 in. I.D. 4-in. diameter spiral tube liquid film capacity coefficient data.**

However, if Heuss had used a longer pipeline, he would have found that the froth flow regime exists only near the distributor and that the true flow regime is slug annular. The annular and mist annular flow data presented by Wales (*15*) appeared to give $k_l a$ values considerably lower than values predicted from our results. The decrease in $k_l a$ with increasing gas velocity (constant liquid velocity) observed by Wales is in complete disagreement with our results. This discrepancy between data is believed to be the result of the experimental technique used by Wales. The rates of desorption of carbon dioxide were measured by withdrawing liquid samples from the center line of the pipe at known distances downstream from the air/water distributor. Sampling at the center line in small diameter pipes is acceptable in the case of slug annular flow, where good radial mixing occurs in the liquid phase. However, in the case of annular or mist annular flow, mass transfer occurs mainly by the interchange of droplets between the gas core and the liquid film on the wall. In most cases, equilibrium is approached between the gas and the liquid droplets in the gas core. Thus the rate of mass transfer must be determined by measuring the solute concentration in the liquid film flowing on the wall of the pipe. On the basis of these observations it was concluded that the data presented by Wales are suspicious and should be used with caution. Comparison of the carbon dioxide-water data of Hayduk (*7*) with our 1-in. pipe data indicated good agreement. A comparison of the mass transfer data of Heuss, Wales, and Hayduk with our results is given in Figure 12. Examination of Hayduk's data on other systems and pipe diameters indicated for each system and pipe diameter satisfactory correlation of the mass transfer data with the frictional energy dissipation. (The two-phase frictional pressure drops used in calculating the frictional energy dissipations were measured values reported in Hayduk's thesis.) A break in the slope of each system's correlation occurred at an energy dissipation of about 0.05 atm./sec. The excellent agreement between Hayduk's data and the results of our study suggests the use of Hayduk's data, in a different way than he used it, to determine the effect of liquid-phase physical properties on $k_l a$. (Hayduk correlated data in the bubble flow regime by means of a multiple regression technique.) Determination of the effect of liquid-phase physical properties was made in the following manner.

The data was assumed to be correlated by two equations, one for $k_l a$ values at energy dissipations of greater

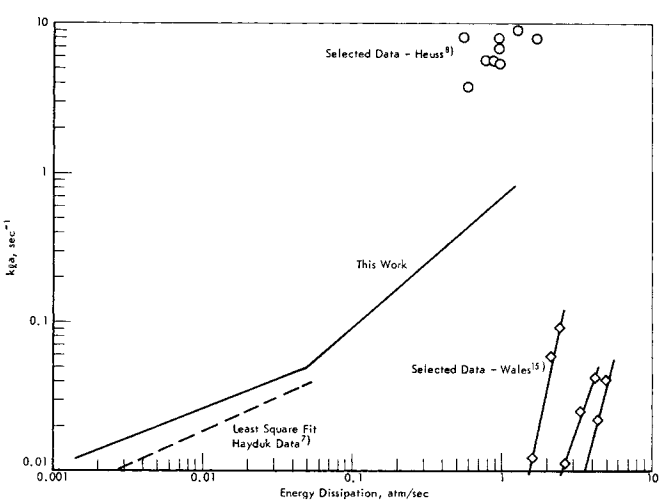


**Fig. 12. Comparison of the 1 in. horizontal pipeline mass transfer data with data available in the literature.**

Table 1. Summary of Experimental Systems Investigated by Hayduk

(7 ft. horizontal pipeline)

| Ref. No. | System | Pipe diameter, in. | Temp, °C. | $V_{SL}$, ft./sec. Max. | $V_{SL}$, ft./sec. Min. | $V_{SG}$, ft./sec. Max. | $V_{SG}$, ft./sec. Min. | $\mu_l$, centipoise | $\rho_l$, lb./cu. ft. | $\sigma$, dynes/cm. | $\mathcal{D}$, sq. cm./sec. $\times 10^5$ |
|---|---|---|---|---|---|---|---|---|---|---|---|
| 1 | Carbon dioxide/water | 0.483 | 15 | 1.74 | 0.50 | 40.1 | 0.20 | 1.14 | 62.4 | 73.5 | 1.465 |
| 2 | Carbon dioxide/water | 0.69 | 15 | 3.6 | 0.52 | 24 | 0.11 | 1.14 | 62.4 | 73.5 | 1.465 |
| 3 | Carbon dioxide/water | 1.00 | 15 | 1.61 | 0.47 | 9.6 | 0.07 | 1.14 | 62.4 | 73.5 | 1.465 |
| 4 | Carbon dioxide/water | 0.69 | 30 | 0.92 | | 18.8 | 0.49 | 0.80 | 62.2 | 71.2 | 2.190 |
| 5 | Carbon dioxide/water | 0.69 | 45 | 0.92 | | 20.9 | 0.19 | 0.60 | 61.8 | 68.8 | 3.08 |
| 6 | Carbon dioxide/ethanol | 0.69 | 13.5 | 1.80 | 0.52 | 20.3 | 0.10 | 1.36 | 49.6 | 23.4 | 2.95 |
| 7 | Helium/water | 0.69 | 15 | 1.80 | 0.52 | 23.9 | 0.13 | 1.14 | 62.4 | 73.5 | 3.69 (5.3)* |
| 8 | Carbon dioxide/glycol | 0.69 | 15 | 1.80 | 0.52 | 18.1 | 0.15 | 26.5 | 69.7 | 49.3 | 0.142 |
| 9 | Carbon dioxide/glycol | 0.69 | 30 | 1.80 | 0.52 | 19.2 | 0.16 | 13.9 | 69.3 | 47.9 | 0.285 |

* More recent value, Vivian, J. Edward, and C. Judson King, *AIChE J.*, **10**, 220 (1964).




Fig. 13. Correlation of mass transfer data.

than 0.05 atm./sec. and the other for $k_la$ values at energy dissipations of less than 0.05 atm./sec. A least-squares fit of Equation (3) was determined for each set of data and was used to represent each system in the determination of the effect of the liquid-phase physical properties. The least-squares fit of Equation (3) to each set of data was used, as some scatter occurred in the experimental data. This scatter occurred mainly under conditions of superficial gas velocities of less than 1 ft./sec. and thus indicates that energy dissipation may not adequately correlate mass transfer data under these conditions. However, at superficial gas velocities of greater than 1 ft./sec., little scatter occurred in the data. Comparison of the resultant equations showed that for energy dissipations of less than 0.05 atm./sec.

$$k_la \sim \epsilon^{\sim 0.4} \tag{4}$$

Similarly, in the high energy dissipation region ($\epsilon \geqq 0.05$ atm./sec.)

$$k_la \sim \epsilon^{\sim 0.8} \tag{5}$$

The lack of dependency of the energy dissipation power constant [constant $B$ in Equation (3)] on the liquid-phase physical properties resulted in all liquid-phase physical property effects being lumped into the constant $A$ in Equation (3). To simplify the following discussion, reference to the various systems studied by Hayduk will be by a reference number. Identification of the system can be made by referring to Table 1 which gives a summary of the systems studied by Hayduk and the corresponding reference number.

The effect of liquid-phase diffusivity on $k_la$ was determined by comparing the equations representing systems 2 and 7. The effect of diffusivity was determined directly, as it was the only liquid-phase physical property that was varied. Results of this comparison indicated that

$$k_la \sim \mathcal{D}^{+0.5} \tag{6}$$

The dependency of $k_la$ on the diffusivity to the 0.5 power is in agreement with both the surface renewal and the Higbie penetration mass transfer models as $a$, the interfacial area, is not dependent on diffusivity.

The effect of surface tension on $k_la$ was estimated by comparing systems 2 and 6. The effect of surface tension in this comparison cannot be determined directly, as differences in liquid viscosity and density occur as well as in surface tension. The difference in diffusivity was eliminated by means of Equation (6). An examination of the percentage change in the physical properties indicated that the change in surface tension was almost a factor of 3

larger than the changes in viscosity and density. On this basis, the deviation between system 2 and 6 was assumed to be the result only of surface tension. Results of this comparison indicated that

$$k_l a \sim (\sigma)^{+0.5} \tag{7}$$

The effect of surface tension given by Equation (7) disagrees with the dispersed flow model, where the maximum stable droplet diameter is determined by a critical Weber number. This disagreement indicates that mass transfer to and from liquid droplets is not controlling. Rather, the critical region is apparently in the liquid film flowing on the wall with increasing surface tension favoring an increase in the film capacity coefficient.

The effect of viscosity of $k_l a$ was estimated by comparing systems 2, 8, and 9. In this comparison it was assumed that the diffusivity and surface tension corrections determined in the preceding sections were valid, and the equations representing systems 2, 8, and 9 were corrected accordingly. With corrections applied for diffusivity and surface tension, the only significant physical property that varied between systems was viscosity. Comparison of systems 2, 8, and 9 indicated that

$$k_l a \sim \mu_l^{0.05} \tag{8}$$

The effect of liquid-phase density was not determined from Hayduk data as the variation in density between systems was insignificant.

The effect of pipe diameter on $k_l a$ for straight horizontal pipes was estimated by comparing systems 1, 2, and 3 of Hayduk's data and the 1 and 4 in. horizontal pipe data obtained in this study. Results of this comparison indicated that for energy dissipations of less than 0.05 atm./sec.

$$k_l a \sim \text{diam.}^{-0.68} \tag{9}$$

For energy dissipations greater than 0.05 atm./sec., $k_l a$ was found to be independent of the diameter. The spiral tube data when corrected by Equation (9) for the effect of diameter agreed reasonably well with the 1 in. horizontal pipe data.

## LIQUID-PHASE CONTROLLED MASS TRANSFER CAPACITY COEFFICIENT CORRELATION

The resultant low ($\epsilon < 0.05$ atm./sec.) and high ($\epsilon \geq 0.05$ atm./sec.) frictional energy dissipation mass transfer correlations are given by Equations (10) and (11), respectively:

$$k_l a \cdot \mathcal{D}^{-0.50} \cdot \sigma^{-0.50} \cdot \mu_l^{-0.05} \cdot \text{diam.}^{0.68} = 3.47\ \epsilon^{0.40} \tag{10}$$

$$k_l a \cdot \mathcal{D}^{-0.50} \cdot \sigma^{-0.50} \cdot \mu_l^{-0.05} = 18.75\ \epsilon^{0.79} \tag{11}$$

Comparison of Equations (10) and (11) with Hayduk's data and the experimental data obtained in our study is shown in Figure 13.

## CONCLUSION

Liquid-phase controlled mass transfer data were correlated with the pipeline two-phase frictional energy dissipation which consists of the product of the two-phase frictional pressure drop and the sum of the superficial gas and liquid velocities. Comparison of measured frictional pressure losses used in the correlation with existing empirical correlations indicated good agreement. A general correlation which includes the effect of liquid-phase physical properties and pipe diameter has been developed for predicting mean liquid-phase film mass transfer capacity coefficients. The ability to predict mass transfer rates from knowledge of only the pressure loss, superficial velocity of each phase and the liquid-phase physical properties provides a means of designing pipeline contactors and reactors which up to the present time has not been possible without extensive experimental studies.


## ACKNOWLEDGMENT

The author would like to acknowledge the valuable assistance of R. W. Lesley and W. B. Schwenning in obtaining the experimental data and the interest and many valuable suggestions given by Dr. G. D. Towell. Permission from Shell Development Company to publish this material is appreciated.


## NOTATION

$\mathcal{D}$ = liquid-phase diffusivity, sq.cm./sec.
diam. = pipe diameter, in.
$G_g$ = superficial gas-phase mass flux, lb.$_m$/(sq.ft.)(sec.)
$G_l$ = superficial liquid-phase mass flux, lb.$_m$/(sq.ft)(sec.)
$k_l a$ = liquid-phase mass transfer film capacity coefficient, sec.$^{-1}$
$p$ = partial pressure oxygen in the liquid phase, mm. Hg.
$p_{\text{air}}$ = partial pressure oxygen in the liquid phase which is in equilibrium with the gas phase in the pipeline, mm. Hg.
$(\Delta P/\Delta L)_{TPf}$ = two-phase frictional pressure drop, lb./(in.$^2$)(ft.)
$V_{SL}$ = superficial liquid velocity, ft./sec.
$V_{SG}$ = superficial gas velocity, ft./sec.
$Z$ = axial location in the pipeline, ft.
$\mu_l$ = liquid-phase viscosity, centipoise
$\rho_l$ = liquid-phase density, lb.$_m$/cu.ft.
$\sigma$ = surface tension, dynes/cm.
$\epsilon$ = energy dissipation = $(\Delta P/\Delta L)_{TPf} \cdot (V_{SG} + V_{SL})/14.7$, atm./sec.

## LITERATURE CITED


1. Anderson, J. D., R. E. Bollinger, and D. E. Lamb, *AIChE J.*, **10**, 640 (1964).
2. Bollinger, R. E., M.S. thesis, Univ. Del., Newark (1960).
3. Calderbank, P. H., and M. B. Moo-Young, *Chem. Eng. Sci.*, **16**, 39 (1961).
4. Cooper, C. M., C. A. Fernstorm and S. A. Miller, *Ind. Eng. Chem*, **36**, 517 (1944).
5. Gill, L. E., G. F. Hewitt, J. W. Hitchon, and P. M. C. Lacey, *Chem. Eng. Sci.*, **18**, 565 (1963).
6. Gill, L. E., G. F. Hewitt, and P. M. C. Lacey, *ibid.*, **19**, 665 (1964).
7. Hayduk, W., Ph.D. dissertation, Univ. British Columbia (1964).
8. Heuss, J. M., C. J. King and C. R. Wilke, *AEC Rept. No. UCRL-11510* (1964).
9. Hughmark, G. A., *Ind Eng. Chem. Fundamentals*, **4**, 361 (1965).
10. Lamont, J. C., and D. S. Scott, *Can. J. Chem. Eng.*, **44**, 201 (1966).
11. Lockhart, R. W., and R. C. Martinelli, *Chem. Eng. Prog.*, **45**, 39 (1949).
12. Perry, J. H., "Chemical Engineer Handbook," 4 ed., Chapt. 14, p. 6, McGraw-Hill, New York (1963).
13. Reiss, L. P., *Ind. Eng. Chem. Process Design Develop.*, **6**, 486 (1967).
14. Scott, D. S., and W. Hayduk, *Can. J. Chem. Eng.*, **44**, 130 (1966).
15. Wales, C. E., Ph.D. dissertation, Purdue Univ., Lafayette, Ind. (1965).
16. White, C. M., *Proc. Roy. Soc. London*, **A123**, 645 (1929).



*Manuscript received May 8, 1968; revision received December 18, 1968; paper accepted December 26, 1968. Paper presented at AIChE Tampa meeting.*